

<https://doi.org/10.15407/ujpe63.8.721>

R. RAJARAMAKRISHNA, Y. RUANGTAWEE, J. KAEWKHAO  
 Center of Excellence in Glass Technology and Materials Science (CEGM),  
 Nakhon Pathom Rajabhat University  
 (Meuang, Nakhon Pathom, 73000, Thailand; e-mail: r.rajaramakrishna@gmail.com)

## Sm<sup>3+</sup>-DOPED MOLYBDENUM GADOLINIUM BORATE GLASSES FOR ORANGE EMISSION LASER ACTIVE MEDIUM

Room temperature visible and near infrared optical absorption and emission spectra of Sm<sup>3+</sup>-doped molybdenum gadolinium borate (MGB) glasses with molar composition 25MoO<sub>3</sub>-20Gd<sub>2</sub>O<sub>3</sub>-(55-x)B<sub>2</sub>O<sub>3</sub>-xSm<sub>2</sub>O<sub>3</sub> (x = 0.05, 0.1, 0.5, 1.0, 2.0 mol.%) have been analyzed. The experimental oscillator strengths of absorption bands have been used to determine the Judd-Ofelt (J-O) parameters. Fluorescence spectra were recorded by exciting the samples at 402 nm. Using the J-O parameters and luminescence data, the radiative transition probabilities (A<sub>R</sub>), branching ratios (β<sub>R</sub>), and stimulated emission cross-sections σ<sub>e</sub> are obtained. The decay curves of the <sup>4</sup>G<sub>5/2</sub>-<sup>6</sup>H<sub>7/2</sub> transition exhibit a non-exponential curve fit for all concentrations. The concentration quenching has been attributed to the energy transfer through the cross-relaxation between Sm<sup>3+</sup> ions. <sup>4</sup>G<sub>5/2</sub> level and its relative quantum efficiencies are measured. Intense reddish-orange emission corresponding to the <sup>4</sup>G<sub>5/2</sub>-<sup>6</sup>H<sub>7/2</sub> transition has been observed in these glasses at the 487-nm excitation. From the values of the radiative parameters, it is concluded that the 1.0-mol% Sm<sup>3+</sup>-doped MGB glass may be used as a laser active medium with the emission wavelength at 599 nm. The analysis of the non-exponential behavior of decay curves through the Inokuti-Hirayama model indicates that the energy transfer between Sm<sup>3+</sup> ions is of dipole-dipole type. The quantum efficiency for the <sup>4</sup>G<sub>5/2</sub> level of MGBSm10 glass is found to be 67%. The co-related color temperature obtained from CIE (Commission International de L'Eclairage) for these glass samples is ~1620 K for the indicated orange emission at the 402-nm excitation.

*Keywords:* trivalent samarium, molecular structure, borate glasses, optical properties, fluorescence spectrum, CIE chromaticity.

### 1. Introduction

Glasses containing rare-earth (RE) ions such as Sm<sup>3+</sup> and Gd<sup>3+</sup> ions have received much attention, because such materials have high potential for practical applications. For instance, Sm<sup>3+</sup>-doped borate glasses have been used as amplifying optical fibers. Because the fluorescence performance of RE ions in glasses depends largely on their site environments (crystal fields), it is of importance to clarify the coordination and bonding states of RE ions in glasses. So far, numerous papers on the optical properties of RE ions in glasses have been reported, and it has been recognized that the Judd-Ofelt analysis is one of the good methods to get information on site environments of

RE ions. MoO<sub>3</sub> is a transition metal oxide, belonging to the intermediate class of glass forming oxides, which may participate in the glass network forming in the presence of modifying oxides with poor metals, but it may also act as a modifier MoO<sub>3</sub>, which is well known as a conditional network former and it is not able to form a glass itself at slow cooling rates. The main problem of the preparation of glasses without involving the network formers is related to a high crystallization tendency of the components. Many binary and more complex molybdate glasses can be obtained by introducing the modifiers or other glass network formers [1-4]. The molybdenum ions exist at least in two stable valence states, viz., Mo(V) and Mo(VI), in the glass network; Mo(VI) ions act as network formers with MoO<sub>4</sub><sup>2-</sup> structural units, alternate with BO<sub>4</sub> structural units, and make the glass network more

© R. RAJARAMAKRISHNA, Y. RUANGTAWEE,  
 J. KAEWKHAO, 2018

ISSN 2071-0194. Ukr. J. Phys. 2018. Vol. 63, No. 8

Table 1. Physical properties of the MGB glass system

Sample Composition	Code	Density (g/cm <sup>3</sup> )	Mol Vol (cm <sup>3</sup> /mol)
25MoO <sub>3</sub> -20Gd <sub>2</sub> O <sub>3</sub> -(55 - x)B <sub>2</sub> O <sub>3</sub> -0.05Sm <sub>2</sub> O <sub>3</sub>	MGBSm0.0	3.9539	37.156
25MoO <sub>3</sub> -20Gd <sub>2</sub> O <sub>3</sub> -(55 - x)B <sub>2</sub> O <sub>3</sub> -0.1Sm <sub>2</sub> O <sub>3</sub>	MGBSm0.1	3.9685	37.055
25MoO <sub>3</sub> -20Gd <sub>2</sub> O <sub>3</sub> -(55 - x)B <sub>2</sub> O <sub>3</sub> -0.5Sm <sub>2</sub> O <sub>3</sub>	MGBSm0.5	3.9747	37.278
25MoO <sub>3</sub> -20Gd <sub>2</sub> O <sub>3</sub> -(55 - x)B <sub>2</sub> O <sub>3</sub> -1.0Sm <sub>2</sub> O <sub>3</sub>	MGBSm1.0	4.0054	37.341
25MoO <sub>3</sub> -20Gd <sub>2</sub> O <sub>3</sub> -(55 - x)B <sub>2</sub> O <sub>3</sub> -2.0Sm <sub>2</sub> O <sub>3</sub>	MGBSm2.0	4.0878	37.270

stable. However, Mo(V) ions may act as modifiers with Mo<sup>5+</sup>O<sup>3-</sup> complexes [5–10].

However, the interest in these glasses is limited as laser hosts due to their high phonon energy. Nevertheless, the addition of a transition metal oxide like MoO<sub>3</sub> to Gd<sub>2</sub>O<sub>3</sub>-B<sub>2</sub>O<sub>3</sub> glass makes it more moisture-resistant, and the phonon losses can also be minimized to a large extent. Further, MoO<sub>3</sub>-Gd<sub>2</sub>O<sub>3</sub>-B<sub>2</sub>O<sub>3</sub> glasses are expected to foster a variety of fluorescence centers, which can be used for the modeling of typical glass applications such as a sensor for the investigation of structural aspects of the amorphous materials [11–12]. MoO<sub>3</sub>-containing glasses have been the subject of many investigations due to their catalytic properties. The ions of molybdenum inculcate high activity and selectivity in a series of oxidation reactions of practical importance in the glass matrices [13]. Gd<sub>2</sub>O<sub>3</sub> has become a material of much interest within the glass matrix because of the highly efficient energy transfer from Gd<sup>3+</sup> ions to incorporated activators, at an affordable cost [14]. While, Gd<sub>2</sub>O<sub>3</sub> has been a popular oxide for photonic materials due to the efficient energy transfer from Gd<sup>3+</sup> ions to luminescence activators, high thermal neutron capture cross-section, and high light yield of emission [15, 16]. Glass scintillators with a high Gd<sub>2</sub>O<sub>3</sub> content are concentrated in various silicate, borosilicate, phosphate, and germanate glasses with fast decay time and/or relative high light yield [17]. The Gd<sup>3+</sup>-RE<sup>3+</sup> energy transfer also can enhance the photoemission, which improves the laser ability. Therefore, it can be said that RE<sup>3+</sup>-doped molybdate gadolinium borate glass is very interesting for using in photonic applications such as a scintillation material and a laser medium. The aim of this investigation is to obtain new molybdate glasses with high concentration of rare-earth oxide Gd<sub>2</sub>O<sub>3</sub> and small concentration of Sm<sup>3+</sup> to make conclusions on the luminescence properties on such concentration inclusions.

## 2. Experimental

The glasses with the compositions of 25MoO<sub>3</sub>-20Gd<sub>2</sub>O-(55 - x)B<sub>2</sub>O<sub>3</sub>-xSm<sub>2</sub>O<sub>3</sub> (x = 0.05, 0.1, 0.5, 1.0, 2.0 mol.%) corresponding sample codes are given in Table 1. The samples were prepared by using the conventional melt quenching technique. The high pure chemicals, MoO<sub>3</sub>, Gd<sub>2</sub>O<sub>3</sub>, H<sub>3</sub>BO<sub>3</sub>, and Sm<sub>2</sub>O<sub>3</sub> with high purity were totally weighted to 30 g, were mixed thoroughly in an alumina crucible, and melted at 1400 °C for 3 h in an muffle furnace. After the melting, the glassy liquid was quenched in preheated graphite mold. The obtained glasses were annealed at 550 °C for 3 h in order to remove thermal strains and then cut and polished for a dimension of 1.0 cm × 1.5 cm × 0.3 cm. The densities of glasses were measured by applying the Archimedes principle. The samples were weighted in air and water on a 4-digit sensitive microbalance (AND, HR 200). The optical spectra were measured with a UV-VI-NIR spectrophotometer (Shimadzu UV-3600) in the ultraviolet, visible, and near-infrared regions. The excitation and emission spectra and the lifetime were collected, by using a spectro-fluoro-photometer (Cary-Eclipse) with a xenon lamp as a light source. The refractive indices (n) were measured by an Abbe refractometer, by using light with a wavelength of 589 nm and 1-Bromonaphthalin as a contact liquid. The absorption spectrum, emission spectrum, and refractive indices were used to analyze the lasing ability of glass via Judd-Ofelt (JO) theory.

## 3. Physical Properties

Density is an effective tool to explore the degree of structural compactness [18], modification of the geometrical configurations of the glass network, change in coordination, and the variation of dimensions of the interstitial holes [19]. It can be seen from Fig. 1 that the density increases with the Sm<sub>2</sub>O<sub>3</sub>

concentration. Eraiah *et al.* (2006) proposed that the addition of a small amount of Sm<sub>2</sub>O<sub>3</sub> which enters into the glass network may resist the creation of nonbridging oxygen [20]. Hence, the density increases with the Sm<sub>2</sub>O<sub>3</sub> content. However, the prepared MGBSm glasses show a decrease in the molar volume under the addition of a very low amount of Sm<sub>2</sub>O<sub>3</sub>, and then it increases along with the density, as the dopant amount increases. This effect suggests an increase of the free space in the glass network. However, the trend of  $r_i$  (interatomic radius) in the prepared glasses decreases the available volume per atom [21]. This implies that the atoms are more tightly packed, resulting in a denser glass, as verified by Table 1. Moreover, the global volume of the network slightly loosens with higher amounts of the dopant (2.0 mol% Sm<sub>2</sub>O<sub>3</sub>). It is expected that the substitution of boron atoms by RE ions with bigger radii, such as samarium, would result in an expansion of the rigid glass structure [22]. Moreover, the dopant ions break the bonds on the network, by promoting the formation of non-bridging oxygens (NBO<sub>s- $\emptyset$</sub> ), thus, resulting in a loosely packed structure [23]. Additionally to this, as shown in Fig. 1, the increase of the molar volume as a function of the Sm<sub>2</sub>O<sub>3</sub> concentration can also be attributed to the formation of BO<sub>3</sub> units linked to Mo<sup>2+</sup> and to the higher bond length of Mo–O than that of the B–O bond.

Table 2. Spectral characteristics of molybdate, gadolinium, and borate groups

Groups	Assignment
<b>Molybdate</b> 760–880 cm <sup>-1</sup>	Stretching vibrations of [MoO <sub>4</sub> ] anions [24–28]
920–980 cm <sup>-1</sup>	Mo–O stretching vibrations of [MoO <sub>6</sub> ] [24–28]
<b>Gadolinium</b> 860–970 cm <sup>-1</sup>	GdB <sub>3</sub> O <sub>6</sub> [29, 30]
<b>Borate</b> [BO <sub>3</sub> ] 1240–1350 cm <sup>-1</sup>	Boroxol rings [26]
[BO <sub>4</sub> ] 900–1100 cm <sup>-1</sup>	Di-, tri-, tetra- and penta-borate groups [26]
720–780 cm <sup>-1</sup>	Oxygen bridges between one tetrahedral and one trigonal boron atom [26]

#### 4. Structural Studies

The structural studies of MoO<sub>3</sub>–Gd<sub>2</sub>O<sub>3</sub>–B<sub>2</sub>O<sub>3</sub> glasses by FTIR reflectance spectra show various reflection bands, which are characteristics of different vibrational modes (see Table 2). The FTIR reflectance spectra of these glasses were recorded in the wavenumber interval 650–1600 cm<sup>-1</sup>, as shown in Fig. 2. The major reflection band centered at ~970 cm<sup>-1</sup> is observed. It arises due Mo–O stretching vibrations and cited as the phonon energy of the present molybdenum glass matrix. The molybdenum

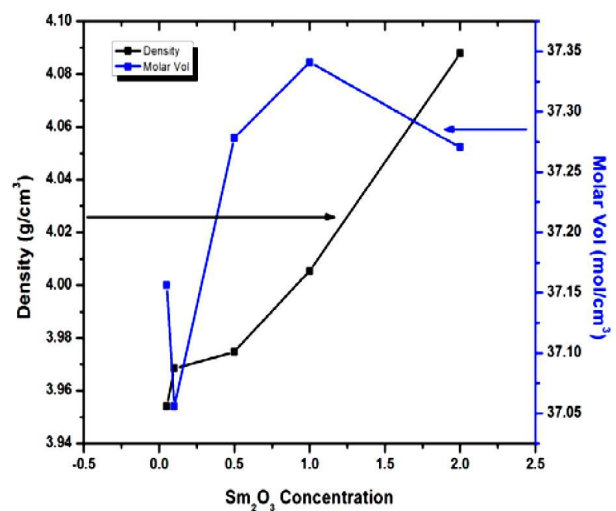


Fig. 1. Density and molar volume versus the concentration of Sm<sup>3+</sup>

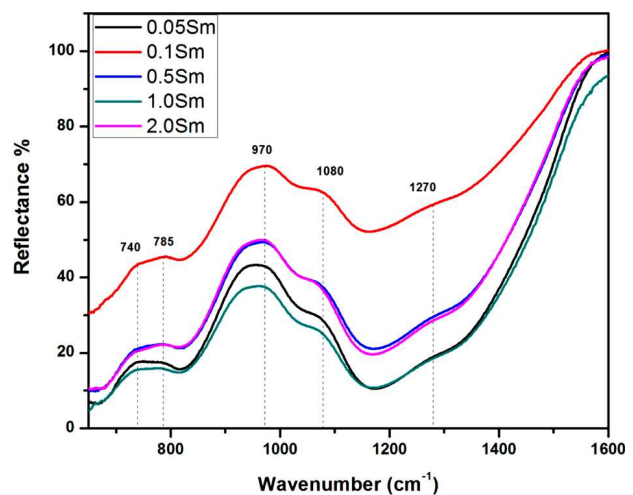


Fig. 2. FTIR reflectance spectra of the Sm<sup>3+</sup>-doped MGB glass system

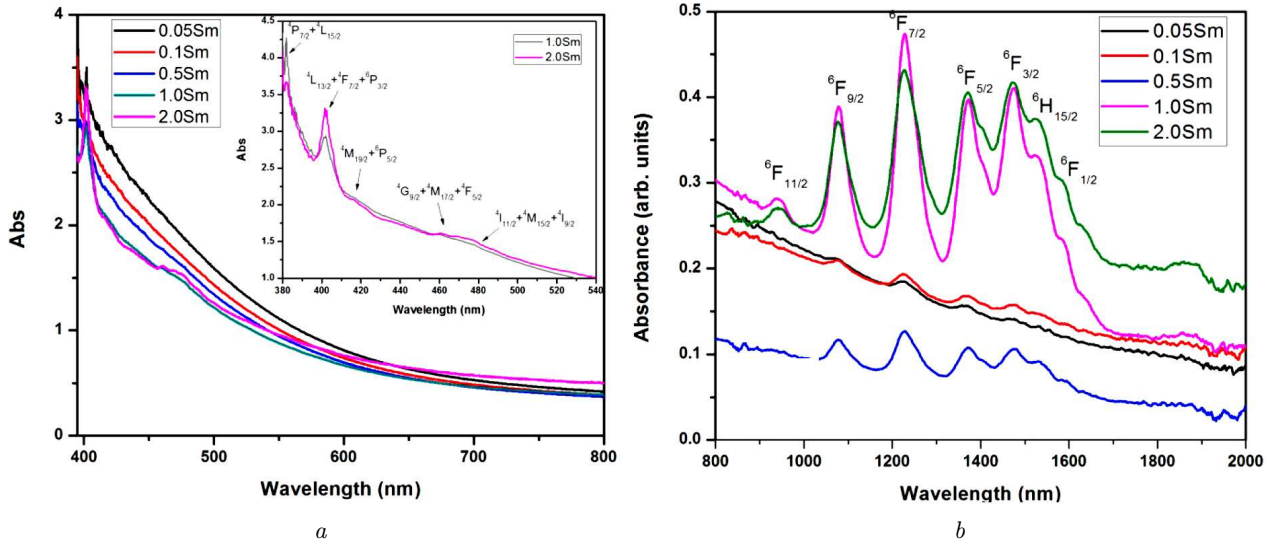


Fig. 3. Optical absorbance spectra for samarium-doped MGB glasses in the UV-Vis region (a) and NIR region (b)

ions can enter the glass network former in position of boron as  $\text{MoO}_4$  and as a network modifier in  $\text{MoO}_6$  groups. In the present system, it is clear from the reflection band that molybdenum ions exist to a large extent as  $\text{MoO}_6$  and are revealed themselves as network modifiers.

### 5. Judd–Ofelt Intensity Parameters

Figure 3, a, b shows the optical absorption spectra of MGB glasses doped with  $\text{Sm}_2\text{O}_3$  in the UV-Vis and NIR regions, respectively. We investigated the optically induced transition and determine the structural properties and J–O intensity parameters. The radiative transitions within the  $4f^n$  configuration of an  $\text{Ln}^{3+}$  ion can be analyzed by the J–O theory [31, 32]. According to it, the calculated oscillator strength,  $f_{\text{cal}}$ , of an induced electric-dipole absorption transition from the initial state ( $\psi J$ ) to a final state ( $\psi' J'$ ) depends on three J–O intensity parameters ( $\Omega_\lambda$ ),

$$f_{\text{cal}} = \frac{8\pi^2 m c v}{3h(2j+1)} \frac{(n^2+2)^2}{9n} \times \sum_{\lambda=2,4,6} \Omega_\lambda (\psi J \parallel U^\lambda \parallel \psi' J')^2, \quad (1)$$

where  $n$  is the refractive index of the medium,  $J$  is the ground-state total angular momentum,  $v$  is the energy of the transition in  $\text{cm}^{-1}$ ,  $\Omega_\lambda$  ( $\lambda = 2, 4, 6$ )

are the Judd–Ofelt parameters, and  $\parallel U^\lambda \parallel^2$  are the squared doubly reduced matrix elements of the unit tensor operator [31–33] of the rank  $\lambda = 2, 4$ , and  $6$ , which are calculated from the intermediate coupling approximation for the transition  $\psi J$  to  $\psi' J'$  at the energy  $\nu$  ( $\text{cm}^{-1}$ ) and are independent of the host. The experimental oscillator strengths ( $f_{\text{exp}}$ ) of the transitions can be obtained by integrating the molar absorptivity ( $\epsilon\nu$ ) at a wave number  $\nu$  ( $\text{cm}^{-1}$ ) for each band as [34]

$$f_{\text{exp}} = 4.32 \times 10^{-9} \int \epsilon(\nu) d\nu. \quad (2)$$

The  $\Omega_\lambda$  parameters have been derived from the electric-dipole contribution of the experimental oscillator strengths, by using the least-square fitting approach. The intensity of an absorption band is determined by its oscillator strength, which is directly proportional to area under the absorption band curve. The experimental oscillator strengths ( $f_{\text{exp}}$ ) obtained from Eq. (2) have been used to determine the J–O intensity parameters by a least-square fit to Eq. (4). The  $\Omega_\lambda$  values thus obtained are used to calculate the theoretical oscillator strengths  $f_{\text{cal}}$ . Table 3 presents the experimental ( $f_{\text{exp}}$ ) and calculated ( $f_{\text{cal}}$ ) oscillator strengths of the observed absorption bands along with *rms* deviations. The small  $\Delta_s$  deviation of  $\pm 0.21 \times 10^{-6}$  between the experimental and calculated oscillator strengths of the absorption bands indicates a good fit. The derived J–O parameters are

Table 3. Experimental and calculated oscillator strengths ( $\times 10^{-6} \text{ cm}^2$ ) of Sm<sup>3+</sup>-doped molybdenum gadolinium borate glasses

Transitions	Energy	MGBSm0.05		MGBSm0.1		MGBSm0.5		MGBSm1.0		MGBSm2.0	
		$f_{\text{exp}}$	$f_{\text{cal}}$	$f_{\text{exp}}$	$f_{\text{cal}}$	$f_{\text{exp}}$	$f_{\text{cal}}$	$f_{\text{exp}}$	$f_{\text{cal}}$	$f_{\text{exp}}$	$f_{\text{cal}}$
<sup>6</sup> F <sub>1/2</sub>	6305.2	0.0364	0.0135	0.0412	0.0245	0.4350	0.3779	0.1900	0.2852	0.1320	0.1864
<sup>6</sup> H <sub>15/2</sub>	6553.1	0.1070	0.0050	0.1640	0.0026	0.2030	0.0017	0.5460	0.0026	0.3070	0.0012
<sup>6</sup> F <sub>3/2</sub>	6775.1	0.2140	0.2271	0.2080	0.1934	0.3300	0.4086	0.6760	0.5256	0.4420	0.3563
<sup>6</sup> F <sub>5/2</sub>	7288.6	0.3970	0.4872	0.2170	0.3941	0.297	0.3126	0.6640	0.7225	0.4690	0.5008
<sup>6</sup> F <sub>7/2</sub>	8143.3	0.8130	0.8880	0.4380	0.5412	0.2970	0.3469	0.6540	0.7047	0.3790	0.4122
<sup>6</sup> F <sub>9/2</sub>	9276.4	0.6890	0.6011	0.4560	0.3271	0.2720	0.2101	0.4190	0.3566	0.2190	0.1774
<sup>6</sup> F <sub>11/2</sub>	10615.7	–	–	–	–	0.1130	0.0040	0.0619	0.0071	0.0513	0.0038
<sup>4</sup> I <sub>11/2</sub> + <sup>4</sup> M <sub>15/2</sub> + <sup>4</sup> I <sub>9/2</sub>	21052.6	–	–	–	–	–	–	0.0679	0.0226	0.2660	0.0085
<sup>4</sup> G <sub>9/2</sub> + <sup>4</sup> M <sub>17/2</sub> + <sup>4</sup> F <sub>5/2</sub>	21739	0.7260	0.1024	0.3970	0.0578	0.1560	0.0369	0.1458	0.0686	0.3339	0.0351
<sup>6</sup> M <sub>19/2</sub> + <sup>6</sup> P <sub>5/2</sub>	23529.4	0.7840	0.1448	0.7280	0.1164	0.0147	0.0711	0.3655	0.1839	0.3065	0.1578
<sup>4</sup> L <sub>13/2</sub> + <sup>4</sup> F <sub>7/2</sub> + <sup>6</sup> P <sub>3/2</sub>	24875.6	1.5900	0.9888	1.8800	0.7942	0.9220	0.4867	0.9024	0.1255	1.4710	1.0766
<sup>4</sup> P <sub>7/2</sub> + <sup>4</sup> L <sub>15/2</sub>	25974.0	–	–	1.0200	0.0143	0.1840	0.0093	0.1782	0.0155	0.1746	0.0058
Transitions		9		10		11		12		12	
$\Delta_{ms}$		0.364		0.526		0.167		0.211		0.200	
RI (n)		1.65450		1.65320		1.65278		1.65257		1.65348	
N (ions/cm <sup>4</sup> )		$1.59 \times 10^{20}$		$3.19 \times 10^{20}$		$1.6 \times 10^{21}$		$3.22 \times 10^{21}$		$6.57 \times 10^{21}$	
$r_p$ (nm)		0.579		0.602		0.352		0.278		0.219	
$r_i$ (nm)		1.850		1.466		0.857		0.678		0.535	

$\Omega_2 = 0.901 \times 10^{20} \text{ cm}^2$ ;  $\Omega_4 = 1.091 \times 10^{20} \text{ cm}^2$ ;  $\Omega_6 = 0.884 \times 10^{20} \text{ cm}^2$ . These J–O parameters are host-dependent and are important for the investigation of the glass structure and the transition rates for rare-earth ion energy levels. The trend of the intensity parameters in the present MGBSm glass is  $\Omega_4 > \Omega_2 > \Omega_6$ , and they are comparable with other reported values in different hosts [35–38] (see Table 4).

In general, the intensity parameter  $\Omega_2$  is related to the covalency, structural change, and symmetry of the ligand field around the Sm<sup>3+</sup> site [39–41]. The  $\Omega_2$  parameter is associated with the asymmetry around the Ln<sup>3+</sup> ion site, while  $\Omega_4$  and  $\Omega_6$  parameters are long-range parameters that can be related to the bulk properties of the glass such as the viscosity and basicity of the matrix. Moreover,  $\Omega_6$  depends on the 6s electron density of Ln<sup>3+</sup> ions [34]. In the present work, the value of the parameter  $\Omega_4$  is higher, refers to the glass matrix viscosity, and is affected by the vibronic transitions of the rare-earth ions bound to the ligand atoms [42].

Table 4. Judd–Ofelt ( $\times 10^{-20} \text{ cm}^2$ ) parameters, trends of  $\Omega_\lambda$  parameters of Sm<sup>3+</sup>-doped molybdenum gadolinium borate glasses

Glass composition	JO Parameters			Trends of $\Omega_\lambda$	Reference
	$\Omega_2$	$\Omega_4$	$\Omega_6$		
MGBSm1.0	0.901	1.091	0.884	$\Omega_4 > \Omega_2 > \Omega_6$	Present
LBTAF	0.27	2.52	2.47	$\Omega_4 > \Omega_6 > \Omega_2$	[35]
ZnBS	0.29	3.82	3.65	$\Omega_4 > \Omega_6 > \Omega_2$	[33]
TeO <sub>2</sub>	3.17	3.65	1.61	$\Omega_4 > \Omega_2 > \Omega_6$	[36]
ZBLAN	2.15	3.05	1.56	$\Omega_4 > \Omega_2 > \Omega_6$	[37]
ZNLAN1	1.95	2.38	1.64	$\Omega_4 > \Omega_2 > \Omega_6$	[38]

The lower  $\Omega_2$  for Sm<sup>3+</sup> ions in these glasses indicates a weaker covalent bonding nature.

### 5.1. Concentration quenching effect on fluorescence spectra

Figure 4, *a* shows the photoluminescence spectra of MGBSm glasses doped with different concentrations of Sm<sup>3+</sup> (0.05, 0.1, 0.5, 1.0, and 2.0 mol%) at room

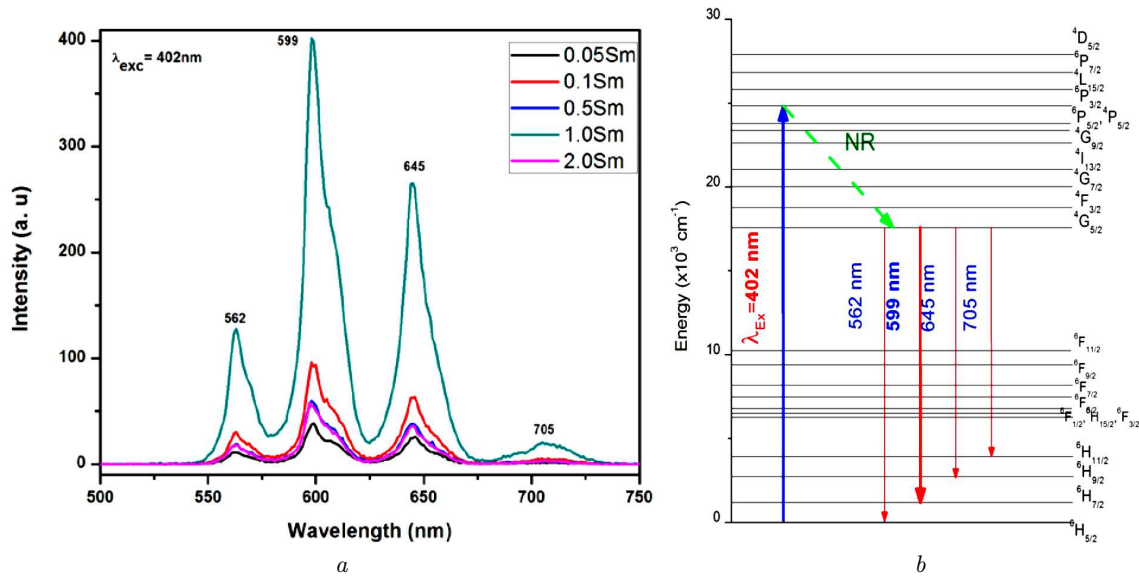


Fig. 4. Room-temperature fluorescence spectra for different concentrations of  $\text{Sm}^{3+}$ -doped MGB glasses (a). Energy level diagrams of  $\text{Sm}^{3+}$ -doped MGB glasses (b)

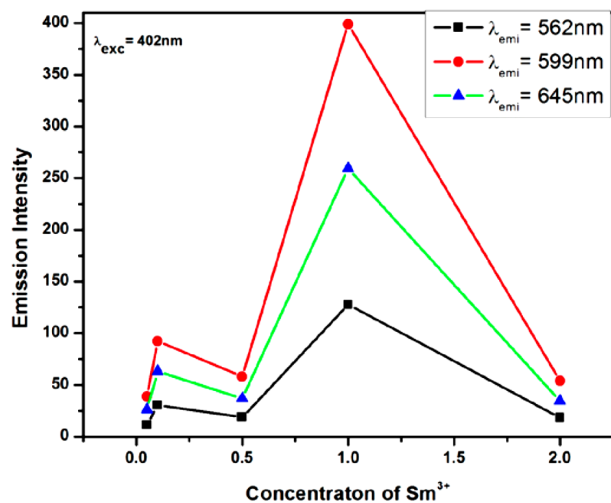


Fig. 5. Fluorescence quenching effect for different concentrations of  $\text{Sm}^{3+}$ -doped MGB glasses

temperature in the spectral interval 500–750 nm with an excitation wavelength of 402 nm corresponding to the  ${}^6\text{H}_{5/2}$ – ${}^4\text{L}_{13/2}$  transition. The fluorescence spectra have been obtained for all the excitation energies higher than  $17.724 \text{ cm}^{-1}$ . The reason for this is that when any of the energy levels above  ${}^4\text{G}_{5/2}$  is excited, there is a quick non-radiative relaxation to this excited level due to the small energy gaps between them. This can be seen from the energy level

of  $\text{Sm}^{3+}$  shown in Fig. 4, b. The  ${}^4\text{G}_{5/2}$  level possesses a purely radiative relaxation rate, since this level has a sufficient energy gap  $\sim 7150 \text{ cm}^{-1}$  with respect to the next lower level  ${}^6\text{F}_{11/2}$  [43]. The fluorescence spectra consist of four peaks and are assigned to the  ${}^4\text{G}_{5/2}$ – ${}^6\text{H}_J$ ,  $J = 5/2, 7/2, 9/2,$  and  $11/2$ , transitions at 562, 599, 645, and 705 nm, respectively. Among these four transitions,  ${}^4\text{G}_{5/2}$ – ${}^6\text{H}_{7/2}$  (599 nm) exhibits the intense orange luminescence, and  ${}^4\text{G}_{5/2}$ – ${}^6\text{H}_{11/2}$  (705 nm) is a feeble one. The other two transitions,  ${}^4\text{G}_{5/2}$ – ${}^6\text{H}_{5/2}$  (562 nm) and  ${}^6\text{H}_{9/2}$  (645 nm), show a moderate luminescence in the visible region. From Fig. 5 presenting the emission intensity, it is very clear that the fluorescence intensity increases with the concentration from 0.05 to 1.0 mol%. Beyond the 1.0-mol%, the concentration quenching is observed. It is also found that the emission peak positions are unchanged for all concentrations.

By the relative areas under the emission peaks, the measured branching ratios ( $\beta_{\text{exp}}$ ) have been estimated for the  ${}^4\text{G}_{5/2}$ – ${}^6\text{H}_J$  ( $J' = 5/2, 7/2, 9/2,$  and  $11/2$ ) transitions, and the results are presented in Table 5. There is a reasonable agreement between measured and calculated branching ratios ( $\beta_{\text{cal}}$ ). As can be seen from Table 5, the  ${}^4\text{G}_{5/2}$ – ${}^6\text{H}_{5/2}$  and  ${}^6\text{H}_{7/2}$  transitions contain the magnetic dipole interaction due to the selection rule  $\Delta J = 0, \pm 1$  [43]. The stimulated emission cross-section ( $\sigma_e$ ) of  $1.19 \times 10^{-22} \text{ cm}^2$  estimated

Table 5. Radiative properties such as the peak emission wavelength ( $\lambda_p$ ), electric and magnetic dipole line strengths ( $S_{ed}$ ,  $S_{md}$ ), transition probability rates ( $A_r$ ), measured branching ratios, and stimulated emission cross-section ( $\sigma_e \times 10^{-22} \text{ cm}^2$ ) for the  ${}^4G_{5/2}$  emission level of the 1.0-mol% Sm<sup>3+</sup>-doped MGB glass

Transition	$\lambda_p$ , nm	$S_{ed}$ , $\times 10^{22} \text{ cm}^{-1}$	$S_{md}$ , $\times 10^{22} \text{ cm}^{-1}$	$A_r$ , S <sup>-1</sup>	Branching ratios		Stimulated emission cross-section ( $\sigma_e$ in cm <sup>2</sup> )
					$\beta_{cal}$	$\beta_{exp}$	
${}^6H_{11/12}$	705	2.43	17.62	10.45	0.0743	0.0069	$3.55 \times 10^{-23}$
${}^6H_{9/2}$	645	39.55	14.60	34.84	0.2478	0.0710	$1.01 \times 10^{-22}$
${}^6H_{7/2}$	599	34.84	0.00	54.15	0.3852	0.1062	$1.19 \times 10^{-22}$
${}^6H_{5/2}$	562	0.00	10.45	20.05	0.1426	0.0282	$4.07 \times 10^{-23}$

for the  ${}^4G_{5/2}$ - ${}^6H_{7/2}$  intense emission band of the 1.0-mol% Sm<sup>3+</sup>-doped MGB glass is comparable with the other reported values [42, 45]. Reasonably high values of  $\sigma_e$  suggest that the present glasses can be used for high-gain laser applications [46–47]. As the intensity of the transition  ${}^4G_{5/2}$ - ${}^6H_{7/2}$  (599 nm) is the highest among all the observed emission transitions, these glasses have inherent favorable local environment to emit the laser output at  $\sim 599$  nm, which is the most prominent and important characteristic of Sm<sup>3+</sup> ions. The support for this viewpoint can be derived from the ratio between the emission state (EM) intensity and the excited state absorption (ESA) intensity. This ratio is calculated in terms of the J–O parameters:

$$\frac{A_{EM}}{A_{ESA}} = 0.21\Omega_6 / (0.11\Omega_2 + 0.063\Omega_4)$$

$A_{EM}/A_{ESA}$  values are found to be 1.106 for MGBSm1.0 glass. As the ratio is higher than unity (this means that  $A_{EM} > A_{ESA}$ ), a light amplification can occur most significantly in the present glasses.

## 6. Lifetime Measurement

Decay curves of the  ${}^4G_{5/2}$  level for different Sm<sup>3+</sup> ion concentrations are shown in Fig. 4. The decay curve is a non-exponential fit for all the samples obtained. The experimental lifetime ( $\tau_{exp}$ ) of the fluorescent  ${}^4G_{5/2}$  level has been determined from the non-exponential decay curves by finding the average or effective lifetime, by using the formula [46, 47]

$$\tau_{exp} = \frac{\int tI(t)dt}{\int I(t)}$$

The measured lifetime (exp) can be expressed as [46, 47]

$$\frac{1}{\tau_{exp}} = \frac{1}{\tau_{rad}} + W_{MPR} + W_{ET},$$

where  $\tau_{rad}$  is the radiative lifetime calculated from the J–O theory,  $W_{MPR}$  is the multiphonon relaxation (MPR) rate,  $W_{ET}$  is the rate of energy transfer (ET). The MPR in this case is negligible, as there is a large energy gap about  $7150 \text{ cm}^{-1}$  between the  ${}^4G_{5/2}$  level and the next lower level. Hence, the quenching of lifetimes with increase in the concentration may be mainly due to ET through the cross-relaxation (CR). The  $W_{ET}$  is given by

$$W_{ET} = \frac{1}{\tau_{exp}} - \frac{1}{\tau_{rad}}$$

$W_{ET}$  (S<sup>-1</sup>) for the  ${}^4G_{5/2}$  level of PPNSm10 glass is found to be  $576 \text{ s}^{-1}$ . The quantum efficiency ( $\eta$ ) of the fluorescent level is given by [48]

$$\eta = \frac{\tau_{exp}}{\tau_{rad}}$$

The quantum efficiency for the  ${}^4G_{5/2}$  level of MGBSm10 glass is found to be 67% and is lower than those obtained for fluorozincate (ZnF<sub>2</sub>-CdF<sub>2</sub>) [49] and higher than those obtained for phosphate PPNSm10 glasses [50]. The luminescence decay curves show the non-exponential nature with the lifetime quenching, when the concentration is increased from 0.05 to 2.0 mol%. The quenching of lifetimes and the non-exponential behavior of decay profiles at concentrations from 0.05 to 2.0 mol% are due to the non-radiative ET between Sm<sup>3+</sup> ions. The intensity of



Table 6. Experimental ( $\tau_{\text{exp}}$ ) & radiative ( $\tau_{\text{rad}}$ ) lifetimes (ms) and the quantum efficiency ( $\eta$ ) of the Sm<sup>3+</sup>:MGB glasses

Sample	$\tau_{\text{exp}}$ ms	$\tau_{\text{rad}}$ ms	$\eta$	Reference
MGBSm0.05	1.071	0.993	1.07	Present work
MGBSm0.1	1.047	1.174	0.89	Same
MGBSm0.5	0.852	0.979	0.87	"
MGBSm1.0	0.571	0.851	0.67	"
MGBSm2.0	0.341	0.892	0.38	"
55P2)5-39PbO-5NbO5-1.0Sm	1.896	2.820	0.69	[50]
49PbO-50GeO2-1.0Sm	1.130	1.653	0.68	[53]
49PbO-30GeO2-20Ga-1.0Sm	1.060	1.740	0.60	[53]
LBSGS2	0.736	0.854	0.86	[34]

of lifetimes decrease with increasing the concentration, and the  $Q$  values shows 0.30 for MGBSm1.0 and 1.5 for MGBSm2.0 samples. The  $C_{\text{DA}}$  values were estimated for the present glasses and are found to be  $0.11 \times 10^{-41}$  cm<sup>6</sup>/s and  $1.1 \times 10^{-41}$  cm<sup>6</sup>/s for MGBSm1.0 and MGBSm2.0, respectively. For Sm<sup>3+</sup>-doped PbO-PbF<sub>2</sub> glass, Nachimuthu *et al.* [52] obtained  $C_{\text{DA}} = 5.6 \times 10^{-41}$  cm<sup>6</sup>/s for 1.35 wt% of Sm<sup>3+</sup> ions. V. Venkatramu *et al.* [43] obtained  $C_{\text{DA}}$  value to be  $4.4 \times 10^{-41}$  cm<sup>6</sup>/s and  $5.3 \times 10^{-41}$  cm<sup>6</sup>/s for 1.5 and 2.5 mol% Sm<sup>3+</sup> ions. All these values are comparable to those obtained for title glass systems.

Usually, in ET processes assisted by phonons, the transfer probability and the  $Q$  parameter are much lower than those in the resonant situation. If the distance between optically active ions decrease (due to an increase in the dopant concentration), then one may expect an increase in the  $Q$  parameter and, as a consequence, faster fluorescence decays. As can be seen, the relative quantum yield exceeds 1 for a lower concentration which is within the experimental error and shows that there is no ET at lower concentrations. Beyond the 0.05-mol% concentration of Sm<sup>3+</sup> ions, ET between Sm<sup>3+</sup> ions has been observed. This is another evidence of ET between Sm<sup>3+</sup> ions in these glasses.

## 7. CIE Chromaticity Analysis

The color chromaticity coordinates  $(x, y) = ((0.59808, 0.39475), (0.60179, 0.39553), (0.60134, 0.39648), (0.60154, 0.39756), (0.59872, 0.39796))$  for MGBSm0.05, MGBSm0.1, MGBSm0.5, MGBSm1.0, and MGBSm2.0, respectively, have been calculated from

the emission spectra gained by the CIE (Commission International de l'Eclairage, France) system and are presented in Fig. 7 for various Sm<sup>3+</sup> concentrations of the doped MGB glasses. The chromaticity coordinates are an evidence supporting the potential analysis of these glasses for the orange emission corresponding to these glass samples. It is not a monochromatic color having a single peak in the spectra, but a mixture of three peaks (562, 599, and 645 nm). The correlated color temperature (CCT) value can be evaluated from the CIE color coordinate, by using the McCamy formula as follows [54–55]:

$$\text{CCT} = -449n^3 + 3525n^2 - 6823n + 5520.33,$$

where  $n = (x - 0.332)/(y - 0.186)$ . The CCT values obtained from the glass samples are  $\sim 1620$  K for these glasses. From these results, it is suggested that the studied glasses emit the orange emission at the 402-nm excitation. Since the ability to withstand a high temperature is a basic requirement for phosphor applied in LEDs, the thermally stable property of phosphor was investigated, and it turned out to be excellent. So, phosphor is a potential orange component for white light-emitting diodes that based on UV-LEDs.

## 8. Conclusions

The present paper reports on the photoluminescence properties of MGB glasses containing different concentrations of Sm<sup>3+</sup> ions. Optical absorption and fluorescence spectra have been recorded at room temperature. The J–O intensity parameters ( $\Omega_\lambda$ ), radiative transition probabilities ( $A_R$ ), branching ratios ( $\beta_R$ ), and stimulated emission cross-section ( $\sigma_e$ )

have been determined and are found to be comparable with other reported values. From the decay curves, it is concluded that the lifetime of the  ${}^4G_{5/2}$  level has been found to depend strongly on the concentration of  $Sm^{3+}$  ions and on the glass composition. The decrease in the lifetime with an increase in the concentrations is due to the cross-relaxation between excited  $Sm^{3+}$  ions and unexcited  $Sm^{3+}$  ions in the ground state. Based on the optical properties, it is concluded that the 1.0-mol%  $Sm^{3+}$ -doped MGB glass may be used as a laser active medium for the emission at 599 nm corresponding to the  ${}^4G_{5/2}$ - ${}^6H_{7/2}$  transition. The analysis of the non-exponential behavior of decay curves within the Inokuti-Hirayama model indicates that the energy transfer between  $Sm^{3+}$  ions is of the dipole-dipole type. The energy transfer parameter ( $Q$ ) and  $C_{DA}$  donor-acceptor interaction parameter increase with the concentration of  $Sm^{3+}$  ions. The CIE chromaticity coordinates  $(x, y) = (\sim 0.601, \sim 0.395)$  are obtained for these glasses, and the CCT values obtained for these glass samples are around 1663 K corresponding to the orange emission at the 402-nm excitation.

*This research work has been supported by the Nakhon Pathom Rajabhat Universty under NPRU research fund (funding project number PD1\_2017).*

- R.G. Gossink. Thesis, Eindhoven O971. *Philips Res. Rep. Suppl.* No. 3. (1971).
- R. Iodanova, V. Dimitrov, Y. Dimitriev, S. Kassabov, D. Kissuski. Glass formation and structure in the system  $MoO_3$ - $Bi_2O_3$ - $Fe_2O_3$ . *J. Non-Cryst. Solids* **231**, 227 (1998).
- Y. Dimitriev, E. Kashchieva, R. Iordanova, G. Tyuliev. Glass formation and microheterogeneous structure in the system  $B_2O_3$ - $V_2O_5$ - $MoO_3$ . *Phys. Chem Glasses* **44**, 155 (2003).
- M. Milanova, R. Iordanova, Y. Dimitriev, D. Klissurski. Glass formation in the  $MoO_3Bi_2O_3$ - $PbO$  system. *J. Mat. Sci. Lett.* **39**, 5591 (2004).
- P. Syam Prasad, B.V. Raghavaiah, R. Balaji Rao, N. Veeraiah. Dielectric dispersion in the  $PbO$ - $MoO_3$ - $B_2O_3$  glass system. *Solid State Commun.* **235**, 132 (2004).
- B.B. Das, R. Ambika. EPR and IR studies on the local structure of  $80MoO_3$ - $20B_2O_3$  glass. *Chem. Phys. Lett.* **370**, 670 (2003).
- L. Bih, E.L. Omari, J.M. Reau, A. Yacoubi, A. Nadori, M. Haddad. Electrical properties of glasses in the  $Na_2O$ - $MoO_3$ - $P_2O_5$  system. *Mater. Lett.* **50**, 308 (2001).
- M. Srinivasa Reddy, V.L.N. Sridhar Raja, N. Veeraiah. Molybdenum ion as a structural probe in  $PbO$ - $Sb_2O_3$ - $B_2O_3$  glass system by means of dielectric and spectroscopic investigations. *EPJ Appl. Phys.* **37**, 203 (2007).
- G. Little Flower, G. Sahaya Baskaran, M. Srinivasa Reddy, N. Veeraiah. The structural investigations of  $PbO$ - $P_2O_5$ - $Sb_2O_3$  glasses with  $MoO_3$  as additive by means of dielectric, spectroscopic and magnetic studies. *Physica B* **393**, 61 (2007).
- G. Srinivasarao, N. Veeraiah. Characterization and physical properties of  $PbO$ - $As_2O_3$  glasses containing molybdenum ions. *J. Solid State Chem.* **166**, 104 (2002).
- C.K. Jayasankar, P. Babu. Optical properties of  $Sm^{3+}$  ions in lithium borate and lithium fluoroborate glasses. *J. Alloys Compd.* **307**, 82 (2000).
- P. Subbalakshmi, B.V. Raghavaiah, R. Balaji Rao, N. Veeraiah. Spectroscopic properties of  $Mo$ - $W$ - $P_2O_5$ :  $Ho^{3+}$  glasses. *EPJ Appl. Phys.* (Fr.) **26**, 169 (2004).
- M. El-Hofy, I.Z. Hager. Ionic Conductivity in  $MoO_3$ - $BaF_2$ - $AgI$ - $LiF$  Glasses. *Phys. Status Solidi A* **182**, 697 (2000).
- J. Kaewkhao, N. Wantana, S. Kaewjaeng, S. Kothan, H.J. Kim. Luminescence characteristics of  $Dy^{3+}$  doped  $Gd_2O_3$ - $CaO$ - $SiO_2$ - $B_2O_3$  scintillating glasses. *J. Rare Earths* **34** (6), 583 (2000).
- Chunmei Tang, Shuang Liu, Liwan Liu, Dan Ping Chen. Luminescence properties of  $Gd^{3+}$ -doped borosilicate scintillating glass. *J. Lumin.* **160**, 317 (2015).
- Z. Onderisinova, M. Kucera, M. Hanus, M. Nikl. Temperature-dependent nonradiative energy transfer from  $Gd^{3+}$  to  $Ce^{3+}$  ions in co-doped LuAG: Ce, Gd garnet scintillators. *J. Lumin.* **167**, 106 (2015).
- Xin-Yuan Sun, Da-Guo Jiang, Wen-Feng Wang, Chun-Yan Cao, Yu-Nong Li, Guo-Tai Zhen, Hong Wang, Xin-Xin Yang, Hao-Hong Chen, Zhi-Jun Zhang, Jing-Tai Zhao. Luminescence properties of  $B_2O_3$ - $GeO_2$ - $Gd_2O_3$  scintillating glass doped with rare-earth and transition-metal ions. *Nucl. Instrum. Methods A* **716**, 90 (2013).
- M.K. Halimah, W.M. Daud, H.A.A. Sidek. *J. App. Sci.* **2340**, 1546 (2005).
- M.R. Raddy, V.R. Kumar, N. Veeraiah. Effect of chromium impurity on dielectric relaxation effects of  $ZnF_2$ - $PbO$ - $TeO_2$  glasses. *Indian J. Pure and Appl. Phys.* **33**, 48 (1995).
- B. Eraiah. Optical properties of samarium doped zinc-tellurite glasses. *J. Indian Acad. of Sci.* **29** (4), 375 (2006).
- Pedro Damas, Joa Coelho, Graham Hungerford, N. Sooraj Hussain. Structural studies of lithium boro tellurite glasses doped with praseodymium and samarium oxides. *Materials Research Bulletin* **47**, 3489 (2012).
- M. Subhadra, P. Kistaiah. Effect of  $Bi_2O_3$  content on physical and optical properties of  $15Li_2O$ - $15K_2O$ - $xBi_2O_3$ - $(65-x)B_2O_3$ :  $5V_2O_5$  glass system. *Physica B* **406**, 1501 (2011).
- Y.B. Saddeek, L.A.E. Latif. Effect of  $TeO_2$  on the elastic moduli of sodium borate glasses. *Physica B* **348**, 475 (2004).

24. E.I. Kamitsos. Infrared studies of borate glasses. *Phys. Chem. Glasses* **44** (2), 79 (2003).
25. A. Mogus-Milankovic, A. Santic, A. Gajovic, D.E. Day. Spectroscopic investigation of MoO<sub>3</sub>-Fe<sub>2</sub>O<sub>3</sub>-P<sub>2</sub>O<sub>5</sub> and SrO-Fe<sub>2</sub>O<sub>3</sub>-P<sub>2</sub>O<sub>5</sub> glasses. Part I. *J. Non-Cryst. Solids* **76**, 325 (2003).
26. M. Rada, S. Rada, P. Pascuta, E. Culea. Structural properties of molybdenum-lead-borate glasses. *Spectrochimica Acta Part A* **77**, 832 (2010).
27. M.S. Reddy, V.L.N. Sridhar Raja, N. Veeraiiah. Molybdenum ion as a structural probe in PbO-Sb<sub>2</sub>O<sub>3</sub>-B<sub>2</sub>O<sub>3</sub> glass system by means of dielectric and spectroscopic investigations. *EPJ Appl. Phys.* **37** (2), 203 (2007).
28. U. Selveraj, K.J. Rao. Role of lead in lead phosphomolybdate glasses and a model of structural units. *J. Non-Cryst. Solids* **104**, 300 (1988).
29. K. Koteswara Rao, M. Vithala, D. Ravinder. Preparation, infrared and magnetic susceptibility studies of LnB<sub>3</sub>O<sub>6</sub> (Ln = Gd, Eu and Sm). *J. Magnetism and Magnetic Materials* **253**, 65 (2002).
30. Okan Icten, Dursun Ali Kose, Birgul Zumreoglu-Karan. Fabrication and characterization of magnetite-gadolinium borate nanocomposites. *J. Alloys and Compounds* **726**, 437 (2017).
31. B.R. Judd. Optical absorption intensities of rare-earth ions. *Phys. Rev.* **127**, 750 (1962).
32. G.S. Ofelt. Intensities of crystal spectra of rare-earth ions. *J. Chem. Phys.* **37**, 511 (1962).
33. C.K. Jayasankar, E. Rukmini. Optical properties of Sm<sup>3+</sup> ions in zinc and alkali zinc borosulphate glasses. *Opt. Mater.* **8**, 193 (1997).
34. R. Rajaramakrishna, B. Knorr, V. Dierolf, R.V. Anavekar, H. Jain. Spectroscopic properties of Sm<sup>3+</sup>-doped lanthanum borogermanate glass. *J. Luminescence* **156**, 192 (2014).
35. B.C. Jamalaliah, J. Suresh Kumar, A. Mohan Babu, T. Sushasini, L. Rama Moorthy. Photoluminescence properties of Sm<sup>3+</sup> in LBTAf glasses. *J. Luminescence* **129**, 363 (2009).
36. L. Boehm, R. Reisfeld, N. Spector. Optical transitions of Sm<sup>3+</sup> in oxide glasses. *J. Solid State Chem.* **28**, 75 (1979).
37. H. Ahrens, M. Wollenhaupt, P. Frobel, J. Lin, K. Barner, G.S. Sun, R. Braunstein. Determination of the Judd-Ofelt parameters of the optical transitions of Sm<sup>3+</sup> in lithiumborate tungstate glasses. *J. Lumin.* **82**, 177 (1999).
38. J. Mc Dougall, D.B. Hollis, M.J.P. Payne. Judd-Ofelt parameters of rare-earth ions in ZBLALi, ZBLAN and ZBLAK fluoride glass. *Phys. Chem. Glasses* **35**, 258 (1994).
39. S. Tanabe, T. Hanada, T. Ohayagi, N. Soga. Correlation between <sup>151</sup>Eu Mossbauer isomer shift and Judd-Ofelt Ω<sub>6</sub> parameters of Nd<sup>3+</sup> ions in phosphate and silicate laser. *Phys. Rev. B* **48**, 10591 (1993).
40. H. Takabe, Y. Nagano, K. Morinaga. Effect of network modifier on spontaneous emission probabilities of Er<sup>3+</sup> in oxide glasses. *J. Am. Ceram. Soc.* **77**, 2132 (1994).
41. S. Tanabe, T. Ohayagi, N. Soga, T. Hanada. Compositional dependence of Judd-Ofelt parameters of Er<sup>3+</sup> ions in alkali-metal borate glasses. *Phys. Rev. B* **46**, 3305 (1992).
42. M. Jayasimhadri, L.R. Moorthy, S.A. Saleem, R.V.S.S.N. Ravi Kumar. Spectroscopic characteristics of Sm<sup>3+</sup>-doped alkali fluorophosphate glasses. *Spectrochim. Acta A* **64**, 939 (2006).
43. V. Venkatramu, P. Babu, C.K. Jayasankar, T. Tröster, W. Sievers, G. Wortmann. Optical spectroscopy of Sm<sup>3+</sup> ions in phosphate and fluorophosphate glasses. *Opt. Mater.* **29**, 1429 (2007).
44. R. Van Deun, K. Binnemans, C. Gorller Walrand. Spectroscopic properties of trivalent samarium ions in glasses. *SPIE* **3622**, 175 (1999).
45. C.K. Jayasankar, P. Babu. Optical properties of Sm<sup>3+</sup> ions in lithium borate and lithium fluoroborate glasses. *J. Alloys Compd.* **307**, 82 (2000).
46. M.B. Saisudha, J. Ramakrishna. Optical absorption of Nd<sup>3+</sup>, Sm<sup>3+</sup> and Dy<sup>3+</sup> in bismuth borate glasses with large radiative transition probabilities. *Opt. Mater.* **18**, (2002) 403 (2002).
47. F. Lahoz, I.R. Martin, J. Mendez-Ramos, P. Nunez. Dopant distribution in a Tm<sup>3+</sup>-Yb<sup>3+</sup> codoped silica based glass ceramic: An infrared-laser induced upconversion study. *J. Chem. Phys.* **120**, 6180 (2004).
48. C. Gorller-Walrand, K. Binnemans. *Handbook on the Physics and Chemistry of Rare Earths*. Edited by K.A. Gschneidner, jr., L. Eyring (North-Holland, 1998), Vol. 25, Chap. 167.
49. V.D. Rodriguez, I.R. Martin, R. Alcalae, R. Cases. Optical properties and cross relaxation among Sm<sup>3+</sup> ions in fluorzincate glasses. *J. Lumin.* **54**, 231 (1992).
50. R. Praveena, V. Venkatramu, P. Babu, C.K. Jayashankar. Fluorescence spectroscopy of Sm<sup>3+</sup> ions in P<sub>2</sub>O<sub>5</sub>-PbO-Nb<sub>2</sub>O<sub>5</sub> glasses. *Physica B* **403**, 3527 (2008).
51. M. Inokuti, F. Hirayama. Influence of energy transfer by the exchange mechanism on donor luminescence. *J. Chem. Phys.* **43**, 1978 (1965).
52. P. Nachimuthu, R. Jagannathan, V. Nirmal Kumar, D. Narayana Rao. Absorption and emission spectral studies of Sm<sup>3+</sup> and Dy<sup>3+</sup> ions in PbO-PbF<sub>2</sub> glasses. *J. Non-Cryst. Solids* **217**, 215 (1997).
53. Eun-Jin Cho, M. Jayasimhadri, Ki-Wan Jang, Gon Kim, Ho-Sueb Lee. Optical spectroscopy and luminescence properties of Sm<sup>3+</sup>-doped lead-germanate glasses. *J. Korean Phys. Soc.* **52**, 599 (2008).
54. L. Mishra, A. Sharma, A.K. Vishwakarma, K. Jha, M. Jayasimhadri, B.V. Ratman, K. Jang, A.S. Rao, R.K. Sinha. White light emission and color tunability of dysprosium doped barium silicate glasses. *J. Lumin.* **169**, 121 (2016).
55. S.N. Rasool, L.R. Moorthy, C.K. Jayasankar. Optical and luminescence properties of Dy<sup>3+</sup> ions in phosphate based glasses. *Solid State Sci.* **22**, 89 (2013).

Received 07.05.18

P. Раджарамакрішна, І. Руангтаві, Дж. Каевхао

СКЛО З БОРАТИВ МОЛІБДЕНУ І ГАДОЛІНІЮ,  
ДОПІЙОВАНЕ  $\text{Sm}^{3+}$ , ЯК АКТИВНЕ СЕРЕДОВИЩЕ  
ЛАЗЕРА З ЕМІСІЄЮ ПОМАРАНЧЕВОГО КОЛЬОРУ

Резюме

Проаналізовано спектри оптичного поглинання і емісії при кімнатній температурі скла з боратів молібдену і гадолінію (МГБ), допійованих  $\text{Sm}^{3+}$  з молярним складом  $25\text{MoO}_3\text{-}20\text{Gd}_2\text{O}_3\text{-(}55-x\text{)B}_2\text{O}_3\text{-}x\text{Sm}_2\text{O}_3$  ( $x = 0,05, 0,1, 0,5, 1,0, 2,0$  мол.%). Експериментальні значення сил осциляторів смуг поглинання використані для визначення параметрів Джадда–Офелта (Дж–О). Записані спектри флуоресценції при збудженні зразків на 402 нм. На основі Дж–О параметрів і даних з люмінесценції, знайдені ймовірності радіаційних переходів ( $A_R$ ), коефіцієнт розпаду ( $\beta_R$ ) і перетини стимульованого випромінювання ( $\sigma_e$ ). Криві розпаду пере-

ходу  ${}^4\text{G}_{5/2}\text{-}{}^6\text{H}_{7/2}$  мають неекспоненціальну залежність для всіх концентрацій. Концентраційні гасіння відповідають переносу енергії між  $\text{Sm}^{3+}$  іонами шляхом крос-релаксації. Визначено  ${}^4\text{G}_{5/2}$  рівень і виміряні його відносні квантові ефективності. Спостерігалось інтенсивне червонувато-оранжеве випромінювання відповідне  ${}^4\text{G}_{5/2}\text{-}{}^6\text{H}_{7/2}$  переходу при збудженні на 487 нм. Виходячи з величин радіаційних параметрів, зроблено висновок про те, що 1,0-мол.%  $\text{Sm}^{3+}$ -допійоване МГБ скло може бути використано як активне лазерне середовище з довжиною хвилі випромінювання 599 нм. Аналіз неекспоненціальних кривих розпаду в моделі Інокуті–Хираяма показує, що перенесення енергії між  $\text{Sm}^{3+}$  іонами має дипольний характер. Отримано, що квантова ефективність для  ${}^4\text{G}_{5/2}$  рівня МГБ Sm10 скла дорівнює 67%. Колірна температура для цих стекел відповідно до даних МКВ (Міжнародна Комісія з висвітлення) дорівнює  $\sim 1620$  К для оранжевого випромінювання при збудженні на 402 нм.